Effect of exhaust stack geometry on the amount of liquid condensate during plant start-up

Rajiv Mongia
Wenjun Qin
Jacques Belanger
Ali Reza

Exponent
5401 McConnell Avenue
Los Angeles, CA 90066

Paolo Zannetti

EnviroComp
2073 Ocaso Camino
Fremont, CA 94539

Liquid condensation on vertical surfaces is a common problem encountered during flue stack operation. Excessive condensation can occur during start-up when the inner surface of the stack is cold. This can lead to re-entrainment of the liquid into the gas stream and subsequent droplet fallout near the stack. The amount of condensate formed during start-up will depend on the properties of the liner and insulation of the stack. In this study, the amount of liquid discharge is quantitatively analyzed for several stack geometries when the temperature of the flue gas is at or above the dew point. Both turbulent deposition and direct film condensation are considered in the modeling. Steady-state condensation due to adiabatic expansion and turbulent deposition onto the wall is quantitatively determined. The direct film condensation is modeled as a transient process, which is relevant under some stack operating conditions such as when the power plant is used for peak demand. A transient, finite difference technique is used to model the stack wall, which is divided into vertical and horizontal sections. The results show that good insulation and proper choice of the liner on the inner surface can significantly reduce the amount of liquid charge during these start-up conditions.

Nomenclature

D diameter of the stack
d_p diameter of the droplet
f friction factor
g gravity at location of chimney
g_0 gravity at sea level
H height of the chimney
h_{fg} the heat of evaporation
k Boltzmann's constant
L height of stack
n_j number of clusters containing j molecules
n_s P_s/kT
Nu_D Nusselt number
Nu_L Nusselt number
P_1 total pressures before the expansion or monomer partial pressure
P_2 total pressures after the expansion
Pr Prandtl number

P_s vapor pressure above a plane surface of liquid
P_{v1} vapor pressures before expansion
P_{v2} vapor pressures after expansion
Re_D Reynolds number
Ra_L Rayleigh number
S P_1/P_s
S_c Schmidt number
Sh_D Sherwood number
T temperature
T_1 temperatures before the expansion
T_2 temperatures after the expansion
U average velocity of gas flow
u_* friction velocity
V deposition velocity
V_+ non-dimensional deposition velocity, V/u_*

γ the ratio of the specific heat at constant pressure to the specific heat at constant volume
μ viscosity of air
ν kinematic viscosity of flue gas
v_m molecular volume of liquid
ρ_{gas} density of the gas
ρ_p density of the droplet
σ surface tension
τ_+ non-dimensional relaxation time

Introduction

Two types of stacks will be discussed in this paper. In "conventional stacks", the flue gases are exhausted at temperatures significantly above their dew point. This is achieved either by exhausting the flue gases without using post-combustion pollution control devices or by "reheating" the flue gases. In either case, condensate will not form in the stack during steady-state operating conditions, although significant condensation can and does occur under cold start-up conditions.

In "wet stacks" the exhaust flue gases are saturated with moisture. A typical wet stack is located downstream from a wet Flue Gas Desulfurization (FGD) system. FGD systems reduce the sulfur dioxide (SO_2) content by spraying a slurry of limestone and lime into the flue gas stream. While SO_2 is scrubbed from the gas stream, water from the slurry saturates the flue gas. In addition, the relatively cool slurry typically reduces the temperature of the flue gas to the range of 45 °C to 55 °C. Since the exhaust stream is saturated with water, condensation will occur in these stacks during steady-state and start-up conditions.

Depending on the operating conditions of the stack and the ambient conditions, there are several sources of liquid condensate within the stack. Typical sources of liquid are:
(1) inefficient removal of droplets within the mist eliminator, (2) adiabatic condensation as

the pressure decreases with height inside the stack, and (3) wall condensation due to temperature and concentration gradients.[1] Whenever condensate is formed, there is also potential for droplet fallout. This occurs when condensed droplets leave the stack and fall to the ground without completely evaporating in the surrounding air. The amount of droplet fallout depends on the gas and liquid flow, heat transfer, and mass transfer that occur within the ductwork and stack.

Small droplets, such as those formed in the exhaust plume, typically evaporate before hitting the ground. However, large droplets, which are sometimes formed by re-entrainment, may fall onto the ground as acid rain and cause corrosion of plant structure, equipment, and vehicles. Re-entrainment is the process where condensate that has collected on the stack wall is sheared off the wall by the flue gases, and is blown out of the stack. This phenomenon is sometimes referred to as "spitting" from the top of the stack. An important consideration in good stack design therefore is to limit the droplet size of the discharged liquid to prevent droplet fallout.

In addition to potential corrosion caused by droplet discharge to surrounding areas, wet acidic flue gas from the FGD can chemically attack the stack liner. Properly selected liner materials and well-designed condensate removal equipment can minimize the corrosion. Commonly used liner materials include acid-resistant brick, closed cell ceramic foams, fiberglass reinforced plastics (FRP), and nickel alloys. Although resistance to corrosion is an important liner property, thermo-physical properties, such as thermal conductivity, specific heat capacity, and density can also greatly affect the heat transfer and mass transfer taking place in the stack. Heat and mass transfer can, in turn, affect the amount of condensate formed on the walls, especially during start-up.

Adiabatic expansion and turbulent deposition

Condensate due to adiabatic expansion and subsequent turbulent deposition is a large contributor to the condensate formed within a stack. Turbulent deposition is the process by which droplets in the free stream migrate and condense onto the surface of the stack. In this research, condensation due to adiabatic expansion is quantitatively determined using a one-dimensional, numerical technique. The extent of turbulent deposition of the condensed droplets onto the walls of typical stacks is then estimated using the flow properties of the flue gases within the stack. For purposes of this analysis, we have assumed that other condensation processes within the stack do not affect either the condensation due to adiabatic expansion or the turbulent deposition. Further, since the temperatures within a wet stack are not substantially above ambient and do not vary significantly from top to bottom, the flue gas is modeled as an ideal gas with constant values of density, thermal conductivity, and heat capacity.

Adiabatic expansion

The static pressure within the stack decreases with the increase of elevation due to the hydrostatic pressure drop. The pressure drop along the height of stack is:[2]

$$\Delta P_H = \frac{g}{g_0} \int_0^H \rho_{gas} dH \tag{1}$$

where g_0 is gravity at sea level, g is gravity at location of chimney, H is height of the chimney, and ρ_{gas} is density of the gas.

The adiabatic expansion process can be described by the expression:[3]

$$\frac{P_1}{P_2} = \left(\frac{T_1}{T_2}\right)^{\frac{\gamma}{\gamma-1}} \tag{2}$$

where P_1, P_2 and T_1, T_2 are the total pressures and temperatures before and after the expansion, and γ is the ratio of the specific heat at constant pressure to the specific heat at constant volume. Since γ is larger than 1 (air is about 1.4, vapor about 1.3), adiabatic expansion leads to a decrease in temperature.

The saturated vapor pressure of the water in the flue gas as a function of temperature can be calculated by the Clausius-Clapeyron equation:

$$\ln\frac{P_{v2}}{P_{v1}} = \frac{h_{fg}(T_2 - T_1)}{RT_2T_1} \tag{3}$$

where h_{fg} is the heat of evaporation, and P_{v1}, P_{v2} and T_1, T_2 are the vapor pressures and temperatures before and after the expansion. The presence of solutes, such as SO_2, can lead to the reduction of the vapor pressure of the water, thereby making it possible for aqueous solution droplets to form in equilibrium with air of relative humidity less than 100%. Since the amount of these solutes will depend on the efficiency of the scrubbing system, the effect of these solutes on the vapor pressure of water was not addressed in this investigation.

Droplet size distribution

The droplet size distribution of the condensed droplets is determined by a combination of thermodynamic and kinetic factors. For this investigation, only the equilibrium thermodynamic effects on the vapor pressure are considered. The droplets are treated as clusters of molecules of a condensable vapor in an inert carrier gas such as air.[3]

$$n_j = n_s S^j e^{\left\{\frac{-3\sigma v_m (\frac{4}{3}\pi / v_m)^{\frac{1}{3}} j^{\frac{2}{3}}}{kT}\right\}} \tag{4}$$

where $S = P_1/P_s$ and $n_s = P_s/kT$, n_j is the number of clusters containing j molecules, P_1 is the monomer partial pressure, P_s is the vapor pressure above a plane surface of liquid, σ is the surface tension, v_m is the molecular volume of liquid, k is the Boltzmann's constant, and T is the temperature in K.

Equation 4 can be simplified as the following by substituting j with droplet volume divided by volume of a single molecule.

$$n_j = n_s S^j e^{\left\{\frac{-3\sigma v_m (\frac{4}{3}\pi/v_m)^{\frac{1}{3}} j^{\frac{2}{3}}}{kT}\right\}} = n_s S^j e^{\frac{-3\sigma v_m (\frac{4}{3}\pi/v_m)^{\frac{1}{3}}(\frac{\frac{1}{6}\pi d_p^3}{v_m})^{\frac{2}{3}}}{kT}} = n_s S^j e^{\left\{\frac{-\sigma\pi d_p^2}{kT}\right\}} \tag{5}$$

Based on the above equation, the number of droplets of size d_p is a function of droplet size, partial pressure, vapor pressure, and temperature. It should be noted that these equations are only valid if there are numerous nucleation sites for condensation to occur and that there is insignificant droplet carryover from the systems upstream of the stack.

Turbulent deposition

Turbulent fluctuation and eddies in the gas flow up the stack provide the mechanism for depositing liquid droplets onto the stack liner surface. Although electrostatic forces, Brownian diffusion, and gravitational forces are also possible mechanisms to create radial velocities, deposition caused by this turbulent motion is the dominant mechanism. The direction of motion in a turbulent flowfield is random, but there is always an outward radial velocity that deposits the droplets on the wall. This radial component of turbulent eddies transports the droplets from eddy to eddy, and eventually to the wall. As a result, a fraction of the droplets in the free stream are deposited onto the wall. This fraction is a function of the geometry of a stack, the velocity of gas flow, and the size of the droplet. For this research, the model developed by Liu and Agarwal[4] is used to calculate the amount of turbulent deposition. Droplet deposition is characterized by deposition velocity and relaxation time. The relaxation time is defined as the time required to bring a moving droplet to rest in a stagnant fluid:

$$\tau = \frac{d_p^2 \rho_p}{18\mu} \tag{6}$$

where d_p is the diameter of the droplet, ρ_p is the density of the droplet, and μ is the viscosity of air. The non-dimensional relaxation time is defined as

$$\tau_+ = \frac{\tau u_*^2}{\nu} \tag{7}$$

where u_* is the friction velocity and ν is the kinematic viscosity of flue gas. The friction velocity is defined as:

$$u_* = \sqrt{f/8} \times U \tag{8}$$

where f is the friction factor and U is the average velocity of gas flow. For flow with a Reynolds number greater than 10^4, the friction factor can be calculated from the following:

$$\frac{1}{\sqrt{f}} = 2.0 \log_{10}(\mathrm{Re}\sqrt{f}) - 0.8, \qquad \mathrm{Re} > 10^4 \tag{9}$$

Equations 6-9 can be used to calculate the non-dimensional relaxation time, τ_+. The relationship between τ_+ and a non-dimensional deposition velocity V_+ ($V_+ = V/u_*$) has been experimentally determined. Substitution of the appropriate deposition velocity for the calculated τ_+ into equation 10 below yields the percentage of deposition:

$$PD = 1 - \exp(\frac{-4LV}{DU}) \tag{10}$$

where L is the height of stack, V is deposition velocity, and D is the diameter of the stack.

Direct Film Condensation

Direct film condensation is the process where condensate will form directly on the relatively cool surface of the stack liner. This mode of condensation is modeled as a transient process using a one-dimensional, finite difference, numerical technique. For this analysis, we have assumed that only a thin film exists at the wall and that other condensation modes do not impact the direct film condensation. The flue gas is assumed to be an ideal gas with constant values of density, thermal conductivity and heat capacity.

Heat transfer from gas phase to the wall

Heat transfer from the gas phase to the wall is calculated by using the Dittus-Boelter equation:[5]

$$Nu_D = 0.023 \, \mathrm{Re}_D^{\frac{4}{5}} \, Pr^n \tag{11}$$

where n = 0.4 for heating and 0.3 for cooling. Nu_D is the Nusselt number, Re_D is the Reynolds number, and Pr is the Prandtl number.

Condensation of water on the wall

Gas flow within the stack is treated as fully developed turbulent flow in a circular tube. The corresponding Dittus-Boelter equation is used to describe the mass transfer in the vicinity of the wall.[5]

$$Sh_D = 0.023 \, \mathrm{Re}_D^{\frac{4}{5}} \, S_c^n \tag{12}$$

where Sh_D is the Sherwood number, Re_D is the Reynolds number, and S_c is the Schmidt number. Equations 11 and 12 have been experimentally verified for a range of conditions:

$$0.7 \le Pr \le 160, \ \mathrm{Re}_D \ge 10000, \ and \ L/D \ge 10 \tag{13}$$

where L is the height of the stack and D is the diameter.

Heat transfer from stack to surroundings

Heat transfer from the stack to the surroundings is treated as convective heat transfer for a cylinder in cross flow. The empirical correlation developed by Hilpert[5] is used.

$$Nu_D = \frac{h_0 D}{k} = C\operatorname{Re}_D^m P_r^{\frac{1}{3}}$$

(14)

where Nu_D is the Nusselt number, Re_D is the Reynolds number, and Pr is the Prandtl number. Constants C and m take different values at different Reynolds numbers.

Natural convection in the air gap

Heat transfer across the air gap (present in some stack geometries) is modeled as natural convection driven by buoyancy created by the temperature difference between the walls. For gaps with a high height to width ratio, the following correlation has been proposed:[5]

$$\overline{Nu_L} = 0.046 R_{aL}^{1/3}$$

(15)

where Nu_L is Nusselt number and Ra_L is the Rayleigh number.

Results and discussion

Stack geometries

Since stack design varies at different installations and environmental conditions are always changing, typical stack geometries with average surroundings conditions are used in this investigation. Tables 1 and 2 summarize typical traditional stack and wet stack geometries, respectively as well as the operating and ambient conditions for the stacks.

Tables 3 and 4 summarize the cross section of a typical traditional stack and wet stack, respectively. Pennguard is a relatively new stack liner material that can be described as a ceramic, closed-cell foam material. It has a low thermal conductivity and heat capacity that results in its ability to heat up quickly when exposed to hot flue gasses and can resist exposure to high temperatures.

Table 1. Overall parameters for a typical traditional stack geometry

Height, m	200
Diameter, m	2.8
Pressure (inlet), bar	1.013
Temperature (inlet), °C	110
Ambient temperature, °C	15
Flow rate, m^3/s	147
Velocity at inlet, m/s	24
Reynolds number	$4.22*10^6$

Table 2. Overall parameters for a typical wet stack geometry

Height, m	200
Diameter (inside), m	6.26
Pressure (inlet), bar	1.013
Temperature (Inlet), °C	47
Ambient temperature, °C	10
Flow rate, m^3/s	615
Velocity at inlet, m/s	20
Reynolds number	$7.9*10^6$

Table 3. Stack geometry for a typical traditional stack

Case	Layer 1	Layer 2
Pennguard	38 mm Pennguard	6 mm carbon steel
Ceramic refractory bricks	100 mm ceramic brick	100 mm foamglass

Table 4. Stack geometry for a typical wet stack

Case	Layer 1	Layer 2	Layer 3	Layer 4	Layer 5
A1	38 mm Pennguard	6 mm carbon steel	1500 mm air gap	300 mm concrete shell	
A2	51 mm Pennguard	6 mm carbon steel	1500 mm air gap	300 mm concrete shell	
A3	38 mm Pennguard	6 mm carbon steel	60 mm glass wool	1500 mm air gap	300 mm concrete
A4	38 mm Pennguard	6 mm carbon steel	100 mm glass wool	1500 mm air gap	300 mm concrete

B	100 mm brick	50 mm foamglass	1500 mm air gap	300 mm concrete	
C	1.6 mm Inconel	6.4 mm carbon steel	100 mm glass wool	1500 mm air gap	300 mm concrete
D	25 mm FRP	60 mm glass wool	1500 mm air gap	300 mm concrete wall	

Adiabatic expansion and turbulent deposition

Figure 1 shows the pressure change caused by the increase in elevation and the temperature change due to adiabatic expansion. The pressure change for a 200 meter stack is about 15 mmHg. The corresponding temperature change is about 2 C.
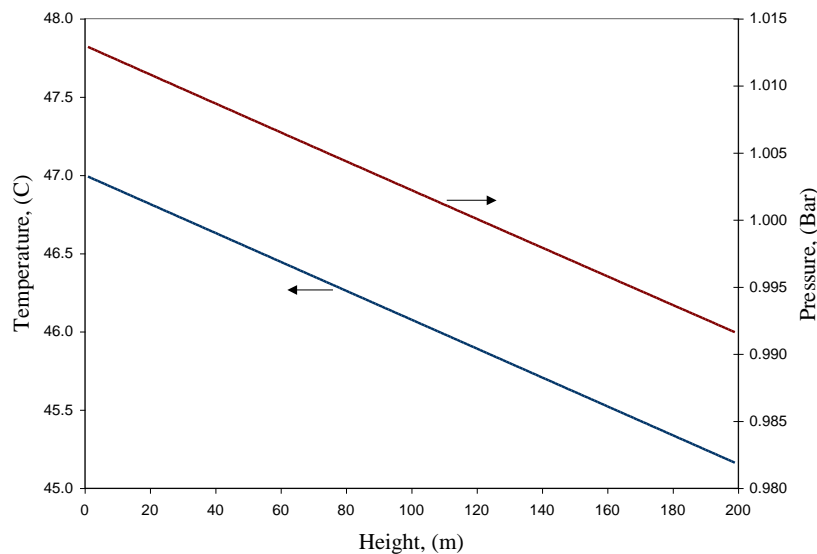
Figure 1. Pressure and temperature changes due to adiabatic expansion

Figure 2 presents the droplet size distribution shown in both number density and mass density. The number density represents the number droplets present of a specific size whereas the mass density represents the mass of droplets present in a certain size range. Although there are a large number of fine droplets, they represent only a small fraction of the total mass. The maximum mass density occurs at a droplet size of 55 μm.
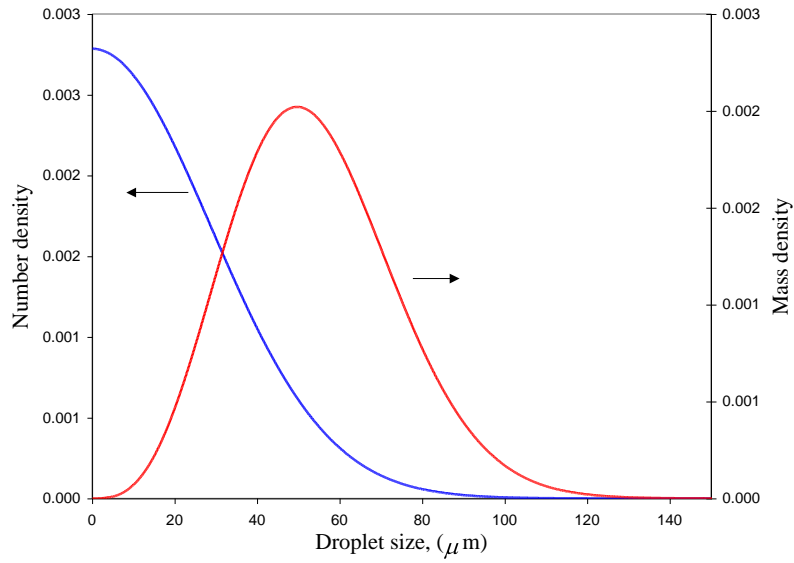
Figure 2. Droplet size distribution

Figure 3 shows the mass of droplets deposited per second, per meter of the stack. The amount of liquid deposited on the wall increases with stack height because there are more droplets at the higher elevations due to the lower temperature.
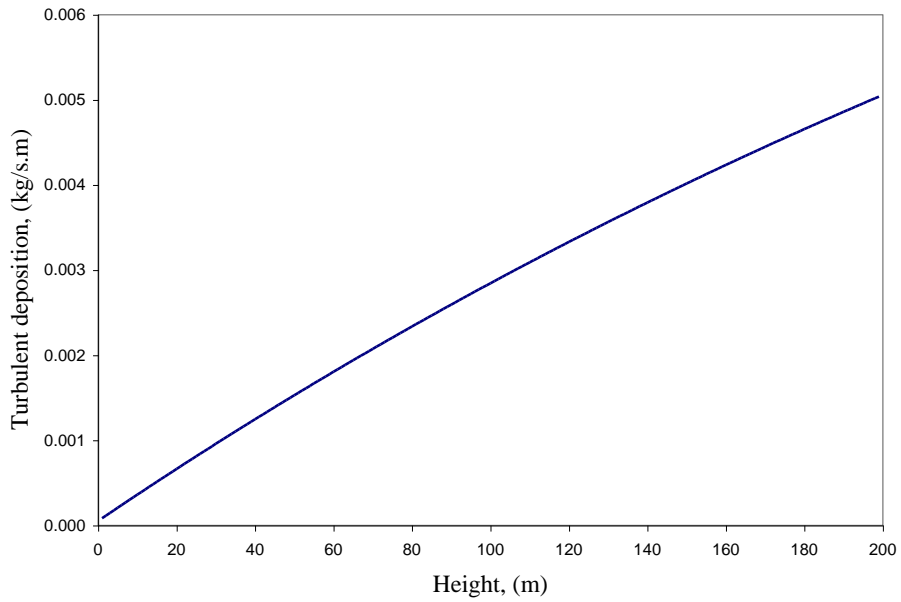
Figure 3. Turbulent deposition along height of stack
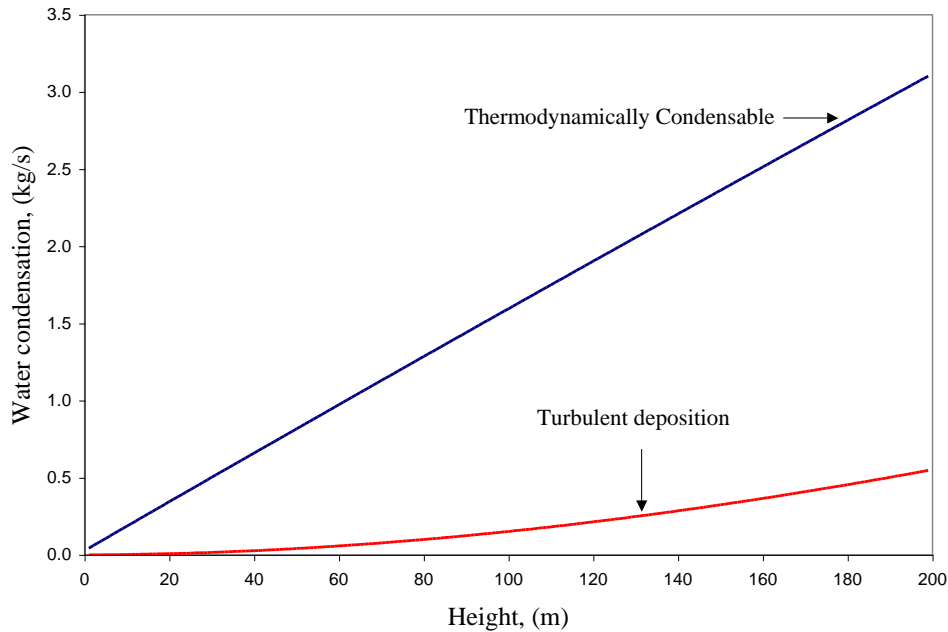
Figure 4. Thermodynamically condensable water and amount of liquid deposited by turbulent deposition along length of stack

Figure 4 shows the thermodynamically condensable liquid water in the stack as a function of height. This water can present itself in droplet form or as a supersaturated vapor. As discussed, more water vapor can condense out with increasing stack height due to adiabatic expansion and consequent reduction in temperatures. Based on this investigation, approximately 17% of the thermodynamically condensable water at the top of the stack was deposited on the wall. This result agrees with earlier research (reference 2) that determined that approximately 5-15% of the droplets smaller than 50 µm would deposit.

Direct film condensation in a wet stack

Figure 5 shows the amount of water condensed as direct film condensation during plant start-up. Water condensation drops significantly during the first 30 minutes due to the rapid heating of the liner material. The initial extent of water condensation is heavily dependent on the thermo-physical properties of the liner material such as thermal conductivity, specific heat and density. Case A has the best performance due to the low heat capacity and thermal conductivity of the Pennguard liner. Case B models a thick (4-inch) brick wall; because of the large thermal mass, it has the lowest surface temperature and highest condensation rate. Case C has thin layers of Inconel and steel and 100 mm of glass wool insulation. Although the surface temperature is initially lower than the flue gas, it eventually increases to a level close to the bulk gas temperature because of the thick insulator behind the liner. As expected, Case D with 25-mm FRP and 60-mm glass wool layers falls in between the two extremes.
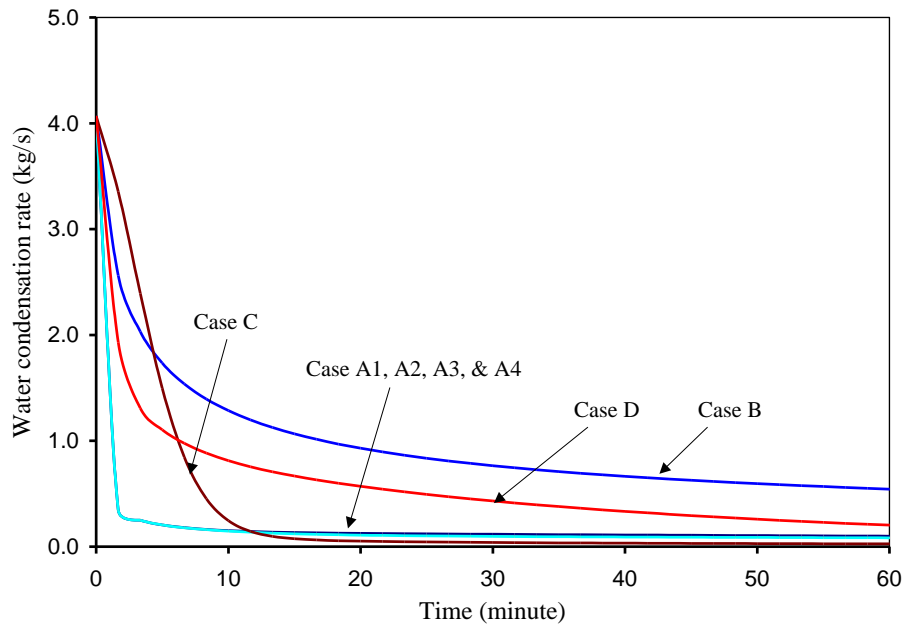
Figure 5. Water condensation due to direct cooling in a wet stack

Figure 6 shows the steady-state temperature profiles across the stack wall (including the air gap and the concrete shell) at the base of the stack. Because all geometries include a 300-mm concrete outer shell (Table 4), the stack with the lowest air gap temperature (horizontal section) would have the lowest heat loss at steady state. Lowering the overall heat loss is critical to reducing water condensation at steady-state.
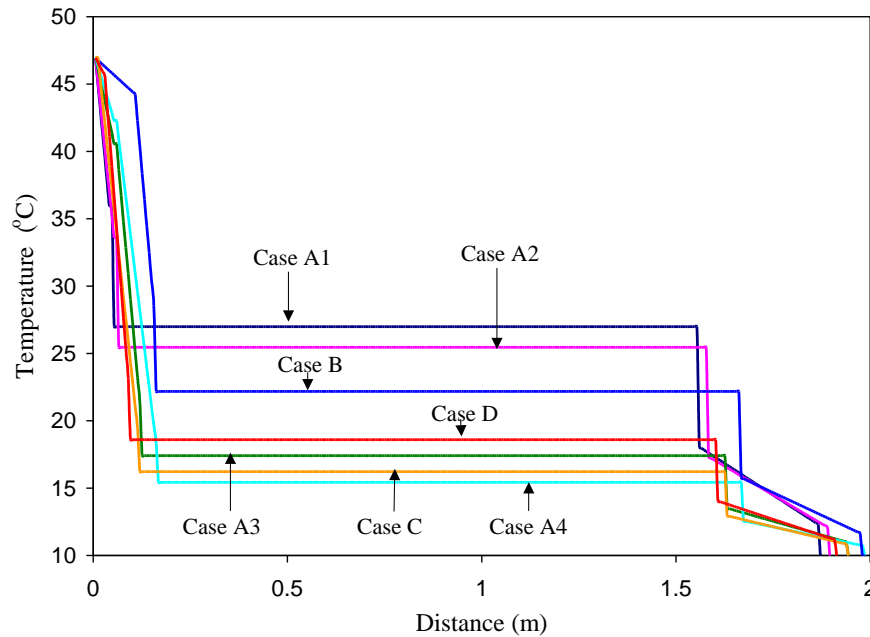
Figure 6. Temperature profiles inside wet stack wall

Direct film condensation in a traditional stack

Figure 7 shows the surface temperature and the condensation rate for the lower portion (the first 40 m) of a chimney constructed of ceramic bricks; wall condensation occurs until approximately 1000 seconds. Figure 8 shows the surface temperature and the condensation rate for the lower portion (the first 40 m) of a chimney constructed with a Pennguard liner; wall condensation only occurs during the first 12 seconds. These results are from the lowest numerical section of the chimney. The other vertical sections exhibit similar results, with expected minor differences in the rate at which the chimney section heats up. Figure 9 shows the cumulative condensate as a function of time for a stack constructed with ceramic bricks and one constructed with a Pennguard liner. Significantly smaller amounts of condensate are formed inside a chimney with the Pennguard liner.
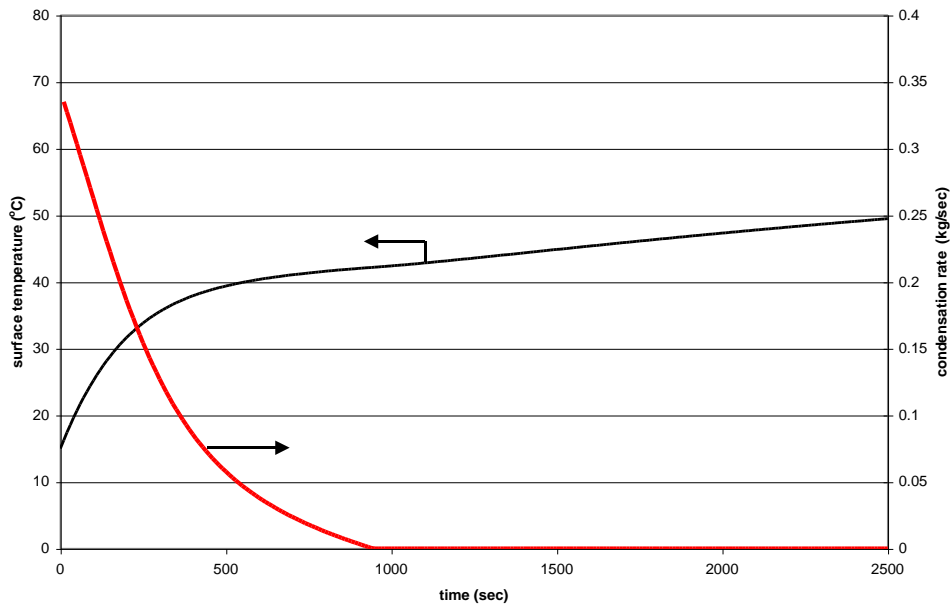
Figure 7. Surface temperature and condensation rate for lower portion (first 40 m) of chimney constructed with ceramic bricks
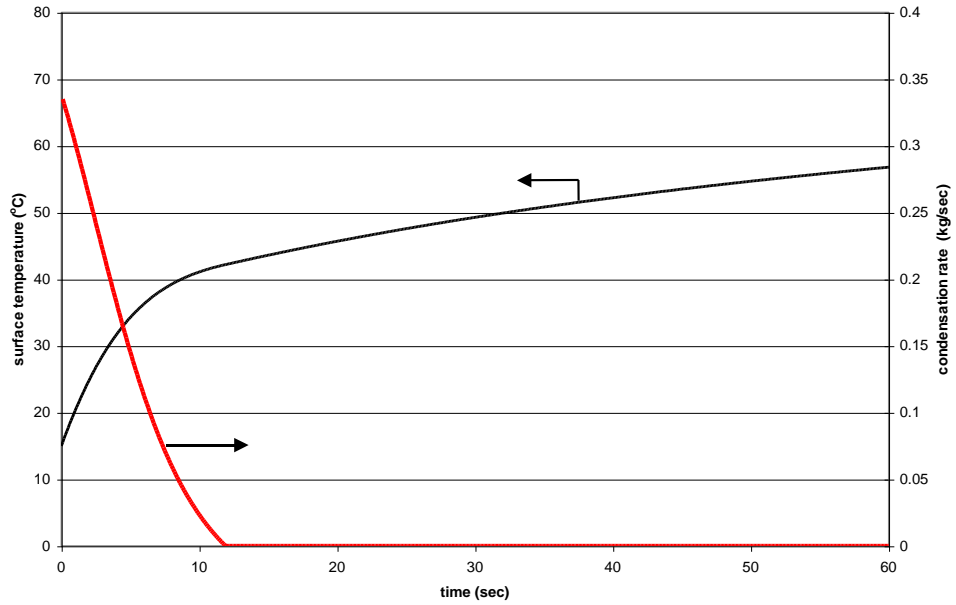
Figure 8. Surface temperature and condensation rate for lower portion (first 40 m) of chimney constructed with Pennguard liner
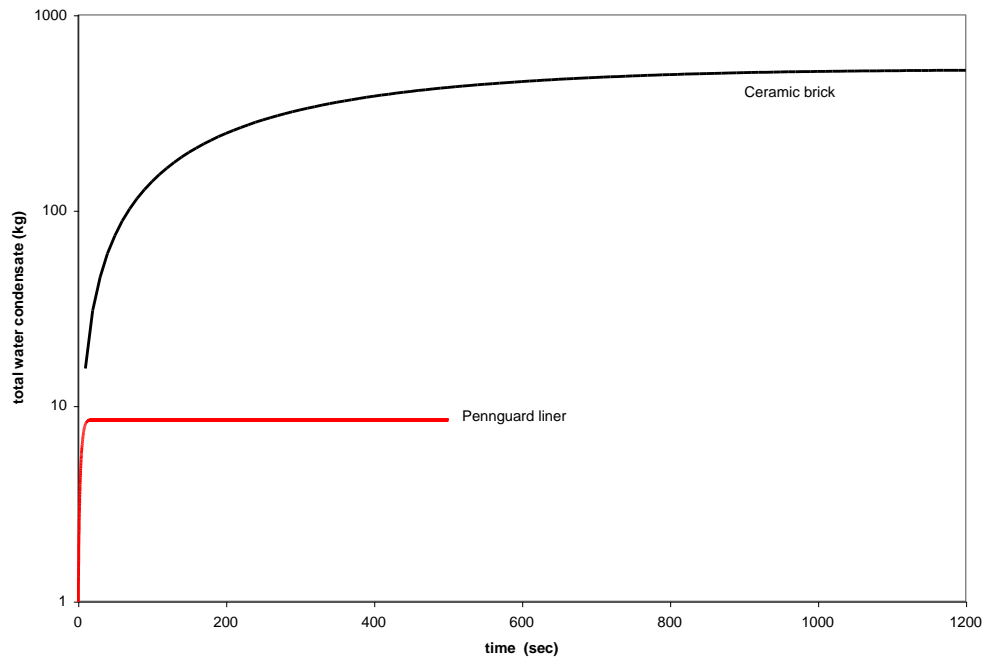
Figure 9. Comparison of total condensate formed during start-up for chimney constructed with ceramic bricks versus chimney with Pennguard liner

14

Conclusions

In this study, we have developed a model to estimate the amount of condensate that collects on the walls of conventional and wet stack geometries. The transient heat transfer model used to calculate film condensation establishes that a significant reduction in water condensation can be achieved if a chimney is constructed with alternate liner materials. This occurs for both traditional and wet stack designs. In wet stacks, appreciable condensation can also occur due to adiabatic expansion and subsequent turbulent deposition. The extent of deposition increases along the height of the stack due to decreasing flue gas temperatures. This analysis as established that for the wet stack case studied, only about 17% of the thermodynamically condensable water is actually deposited on the walls near the top of the stack.

This investigation shows that careful selection of liner materials and insulation can have a significant impact on the amount of condensate collected on the walls of a stack. While the ultimate fate of the condensate (re-evaporation, entrainment into the exhaust stream, or collection at the bottom of the chimney) would require a more detailed analysis and is dependent on the specifics of the installation of interest, this work has identified a possible method for reducing the amount of total condensate.

Acknowledgements

References

1. Rosenberg, H.S. *Power Engineering,* 1998, 102, 76-82.

2. Dynatech R/D Company, *Entrainment in Wet Stacks. Final Report*; U.S. Department of Commerce, National Technical Information Service DE82906487, 1982.

3. Friedlander, S.K. *Smoke, Dust and Haze, Fundamentals of Aerosol Behavior*, John Wiley & Sons, 1977.

4. Liu, B.Y.H. and Agarwal, J.K, *Aerosol Science,* 1974, 5, 145-155.

5. Incropera, F.P. and DeWitt, *Fundamentals of Heat and Mass Transfer*, 4th ed, John Wiley & Sons.